

PLATE 1: GEOLOGIC MAP OF PELONA SCHIST ON CENTRAL BLUE RIDGE, EASTERN SAN GABRIEL MOUNTAINS, SOUTHERN CALIFORNIA

(Compiled from mapping by Manker and Nourse, 2018-2022; Nourse, 1993, 2001; Nourse with GSC 5030L and GSC 4910L students, 2013; Ehlig and Dibblee, 1967; Dibblee and Minch 2002; Coffey et al., 2019)

Base Maps: USGS (US topo) Mescal Creek and Mount San Antonio, Ca 7.5' Quadrangles, 2018

LEGEND

	Fill Color
	Observed Outcrop
	Grayschist - muscovite rich
	Grayschist - chlorite rich
	Grayschist - weathers yellowish brown
	Greenschist - actinolite rich
	Calc-silicate gneiss
	Mafic schist - hornblende rich
	Spotted mafic schist
	Banded grayschist - mscovite rich
	Banded grayschist - chlorite rich
	Banded greenschist - actinolite rich
	Metachert
	N/A Pelona schist of Blue Ridge (undifferentiated)
	JNCM1947 Detrital zircon sample
	JN2058 Thin section sample
	Foliation (Nourse and Manker 2018-2022; Nourse and students, 1993-2013)
	Overturned fold (synform or antiform)
	Fault trace
	North-trending syn-metamorphic fold hinge: Late Cretaceous-early Tertiary
	West-northwest-trending Miocene(?) fold hinge
	Stereonet Compilations from Sub-Areas Stereonets with axial planes = Fold solution with axial plane and poles to foliations; trend and plunge of fold hinge
	Stereonets without axial planes = poles to foliation of boxed area

Previous Work (Incorporated)

	Quaternary alluvium (undifferentiated)
	Pg-eNg Vasquez Formation (undifferentiated)
	Mylonite
	Mesozoic granitic intrusive
	BR218 and 98-240 Detrital zircon sample (Grove et al, 2003; Jacobson et al, 2011)
	Foliation (Dibblee, 1967; Elig, 1967 - unpublished)
	Foliation (Dibblee and Minch, 2002 - measured)
	Foliation (Dibblee and Minch, 2002 - approximated?)
	Overturned fold (Dibblee and Minch, 2002)
	Plunging Anticline (Dibblee and Minch, 2002)

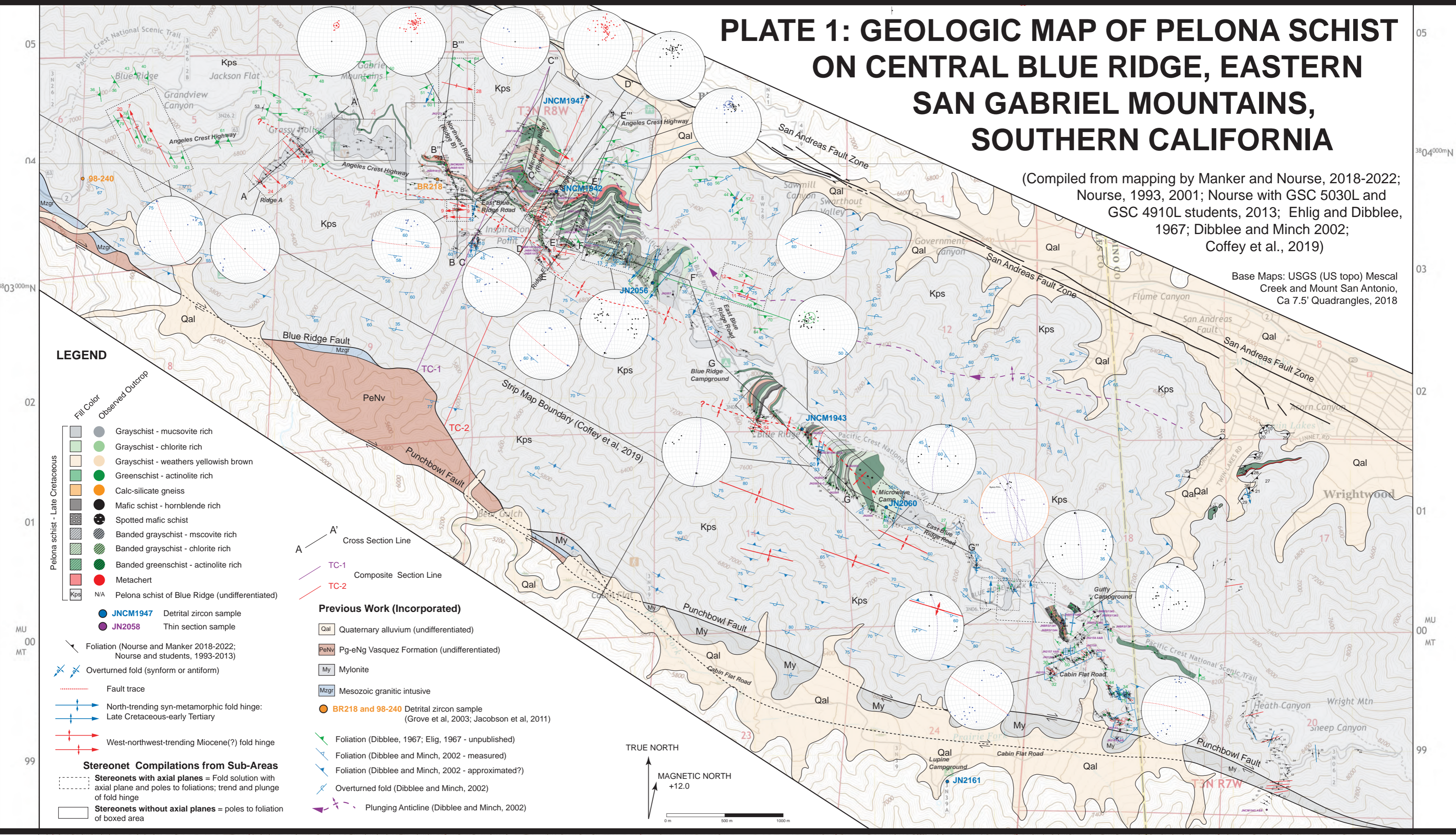
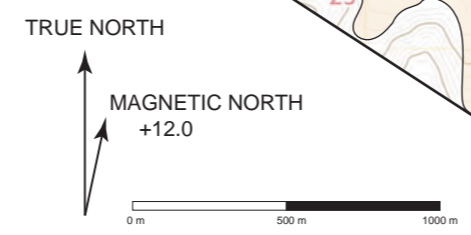
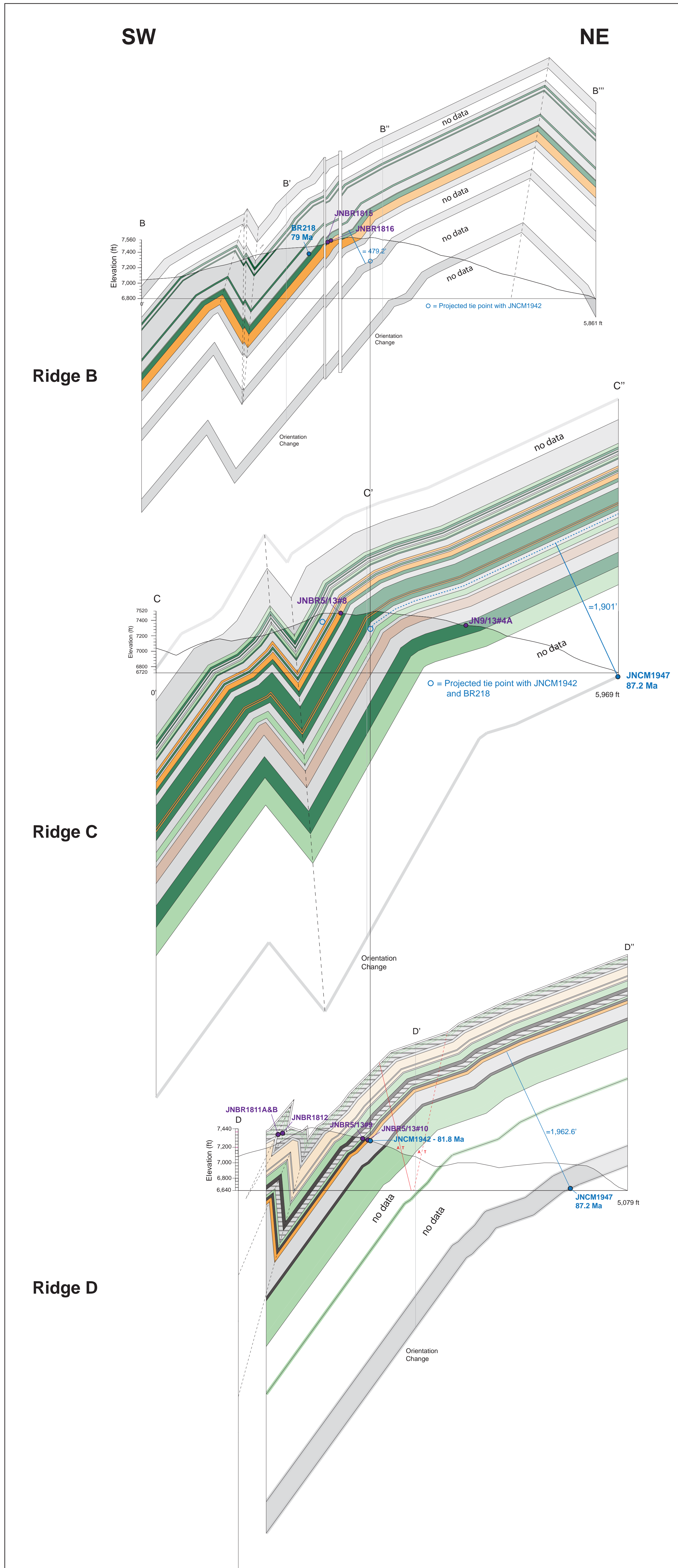


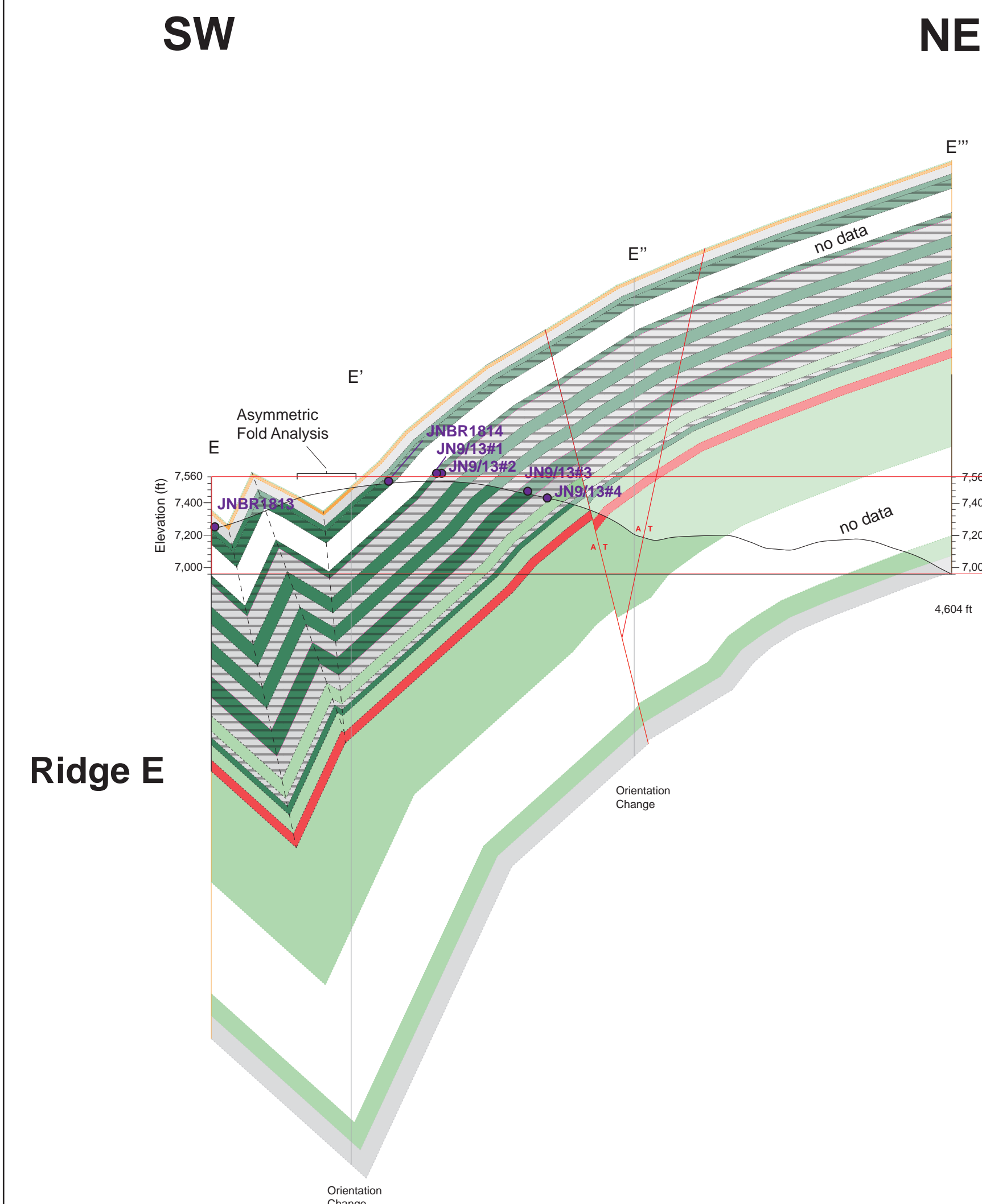
PLATE 2: CROSS-SECTIONS AND GEOCHRONOLOGY SECTIONS OF PELONA SCHIST ON CENTRAL BLUE RIDGE, EASTERN SAN GABRIEL MOUNTAINS, CALIFORNIA, USA



Composite Geochronology Section 1 (Cross-Sections B, C, D)

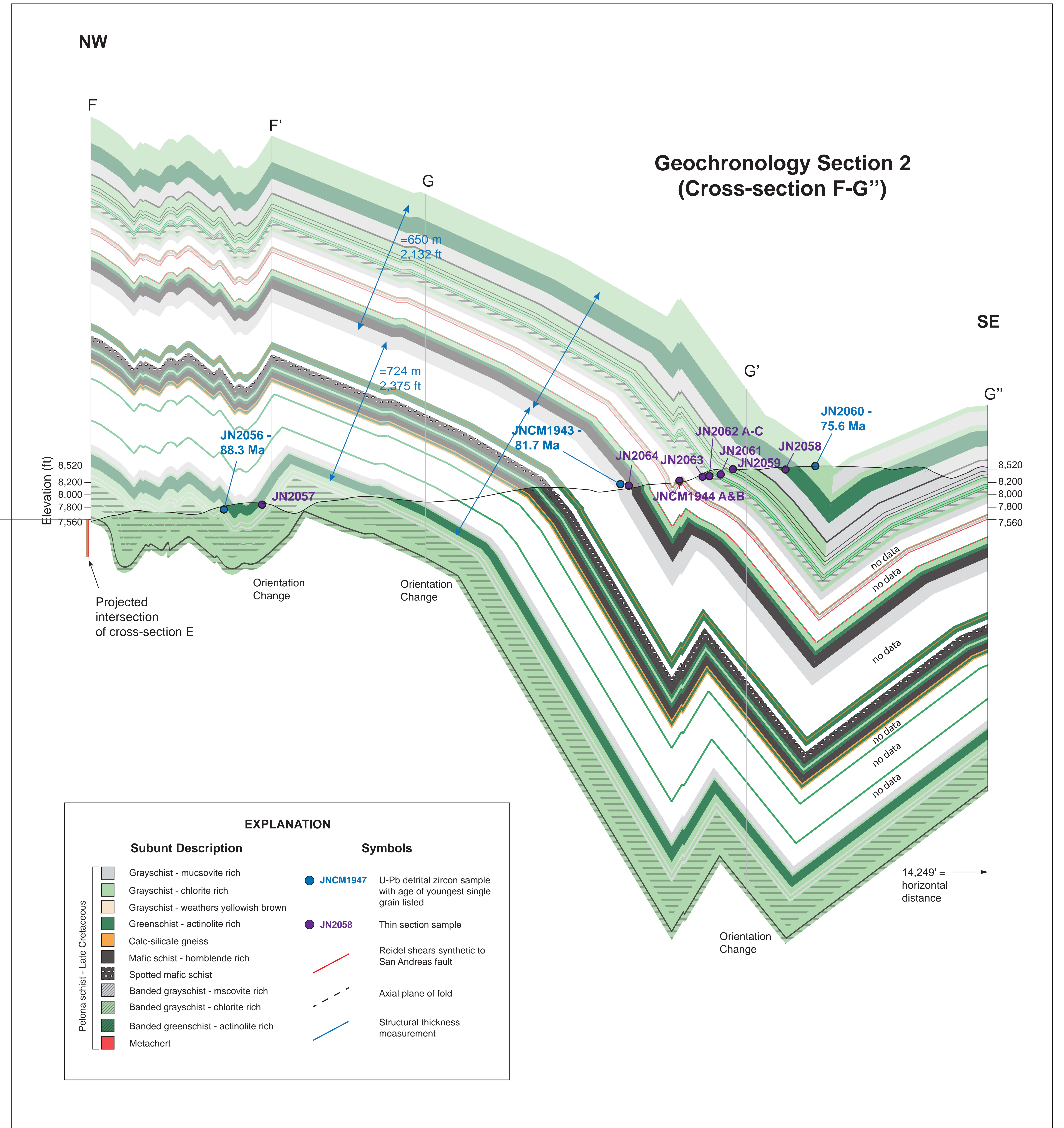
Ridges B, C, and D were tied together in plan view by projecting a line from geochronology sample site JNCM1942 (cross-section D) along mapped changes in strike to cross-section C and then to cross-section B. Cross-sections to the left are arranged SW to NE by a vertical tie line which corresponds to the horizontal tie line points discussed above.

Note: Cross-section A was not completed in this study due to time constraints, as this section presented no significant contribution other than fold geometry.



CROSS-SECTION CONSTRUCTION METHODS

Cross-sections were constructed with the goal of maintaining subunit thickness throughout folding to ensure the accurate measurement of structural thickness between geochronology samples. Methods used in construction included: 1) the calculation of apparent dips for all structural measurements not perpendicular to the cross-section line. 2) Axial planes of folds were determined by bisecting the angle between apparent dip reversals. 3) Large scale shallow curvature of the sections were determined geometrically by bisecting the change in dip angle values and determining an axial plane angle of the curvature. This ensured that subunit thickness could be maintained. As the goal of balanced geometry of the cross-sections for this study was achieved, cross-sections were left angular due to time constraints.



EXPLANATION	
Subunit Description	Symbols
Grayschist - muscovite rich	JNCM1947 U-Pb detrital zircon sample with age of youngest single grain listed
Grayschist - chlorite rich	JN2058 Thin section sample
Grayschist - weathers yellowish brown	Reidel shears synthetic to San Andreas fault
Greenschist - actinolite rich	Axial plane of fold
Calc-silicate gneiss	Structural thickness measurement
Mafic schist - hornblende rich	
Spotted mafic schist	
Banded grayschist - muscovite rich	
Banded grayschist - chlorite rich	
Banded greenschist - actinolite rich	
Metachert	

JN2161-55	318.9412	1.797114	4.321825	0.19831	0.303172	0.010126	0.386480832	3.326103	0.114943	0.103404	0.004398	0.359062275	1690	18	1695	26	1685	39	1685	39	-0.3	-0.6
JN2161-49	82.7544	1.346032	3.891658	0.164477	0.280122	0.011531	0.268535123	3.612488	0.149379	0.103436	0.005095	0.576445045	1623	17	1575	29	1686	45	1686	45	3.0	6.6
JN2161-35	918.381	16.08016	3.731085	0.218277	0.268402	0.02073	0.678481838	3.888427	0.309447	0.103798	0.006276	0.555596595	1567	27	1475	52	1692	56	1692	56	5.9	12.8
JN2161-50	352.5757	2.668817	4.359558	0.13524	0.310078	0.010263	0.236995173	3.250905	0.112905	0.104014	0.004133	0.657167724	1714	13	1729	26	1696	37	1696	37	-0.9	-1.9
JN2161-45	512.634	2.251627	4.931668	0.24858	0.339003	0.010341	0.622664287	2.946068	0.104597	0.104065	0.004118	0.049908994	1797	22	1884	29	1697	36	1697	36	-4.8	-11.0
JN2161-38	250.8509	2.673761	4.772438	0.210832	0.331539	0.016769	0.491583597	3.071758	0.152695	0.104259	0.004965	0.557418296	1763	19	1817	39	1700	44	1700	44	-3.1	-6.9
JN2161-73	168.469	2.131436	4.326552	0.144122	0.300302	0.008045	0.666383946	3.346895	0.087403	0.104485	0.002673	0.22091246	1694	13	1685	19	1704	24	1704	24	0.5	1.1
JN2161-69	442.8744	4.224192	3.830069	0.141389	0.263252	0.007496	0.494920879	3.789714	0.125806	0.104515	0.003662	0.489753063	1593	14	1510	22	1705	32	1705	32	5.2	11.4
JN2161-59	1462.741	14.56801	4.050876	0.180138	0.2773	0.011112	0.523530806	3.647515	0.143771	0.106457	0.004781	0.204685223	1639	22	1562	27	1739	41	1739	41	4.7	10.2
JN2161-64	274.8668	1.902701	4.106792	0.146606	0.275064	0.008248	0.535308426	3.660042	0.113467	0.107356	0.003466	0.300436183	1643	15	1557	21	1754	30	1754	30	5.2	11.2
JN2161-74	1890.468	1.112872	4.641524	0.148901	0.315219	0.012732	0.422044628	3.20821	0.123248	0.107467	0.004158	0.673936069	1752	13	1749	29	1756	35	1756	35	0.2	0.4
JN2161-63	1388.918	7.21574	4.180374	0.214492	0.279793	0.016021	0.680667007	3.661093	0.21198	0.107988	0.004762	0.465807328	1647	22	1557	40	1765	40	1765	40	5.5	11.8
JN2161-62	1891.251	3.761258	4.389896	0.187626	0.289493	0.012229	0.671865891	3.498752	0.146336	0.109006	0.00362	0.323022349	1692	18	1621	30	1782	30	1782	30	4.2	9.0
JN2161-24	875.3529	9.558061	4.969552	0.468429	0.310618	0.022435	0.937794755	3.305662	0.173939	0.112536	0.004002	-0.14724799	1766	28	1704	39	1840	32	1840	32	3.5	7.4
JN2161-72	468.1588	4.33983	10.16818	0.3301	0.444458	0.011893	0.507205698	2.261967	0.064477	0.165983	0.004987	0.371748735	2445	15	2360	28	2517	25	2517	25	3.5	6.2
JN2161-57	1225.551	4.154561	10.32899	0.522161	0.436933	0.016791	0.606381034	2.311962	0.087132	0.170337	0.00723	0.139470337	2449	24	2317	37	2560	36	2560	36	5.4	9.5

ⁿ Data not corrected for common-Pb.

[†] ²⁰⁶Pb/²³⁸U ages common lead corrected by inferring the initial Pb-composition from the Stacey and Kramers (1975) two stage isotope evolution model (Vermeesch, 2018). Analyses with greater than 10% uncertainty in ²⁰⁷Pb/²⁰⁶Pb age (1-sigma) or 5% uncertainty in ²⁰⁶Pb/²³⁸U age (1-sigma), 20% discordance, and/or 5% reverse discordance are excluded. Accepted ages calculated using ²⁰⁶Pb/²³⁸U ages for grains younger than 1100 Ma and ²⁰⁷Pb/²⁰⁶Pb ages for grains older than 1100 Ma.